UNIVERSITI TEKNOLOGI MARA

University Publication Centre (UPENA)

Journal of Mechanical Engineering

Faculty of Mechanical Engineering

Volume 3 No. 1 June 2006 ISSN 1823-5514

JOURNAL OF MECHANICAL ENGINEERING
(JMechE)

© Journal of Mechanical Engineering (ISSN 1823-5514) is jointly published by the Faculty of Mechanical Engineering (FKM) and Pusat Penerbitan Universiti (UPENA), Universiti Teknologi MARA, 40450 Shah Alam, Selangor, Malaysia.

Correspondence Address:

The Dean
Faculty of Mechanical Engineering
Universiti Teknologi MARA
40450 Shah Alam, Malaysia.
Tel: 603- 5543 5161
Fax : 603- 5543 5160
Email : aro@salam.uitm.edu.my;
aidahjumahat@salam.uitm.edu.my

Journal of Mechanical Engineering

Faculty of Mechanical Engineering

Volume 3 No. 1 | June 2006 | ISSN 1823-5514

Fracture Behaviour of Metal Powder Compact

S.M. Tahir, A.K. Ariffin & N. Muhamad

ABSTRACT

This paper is intended to establish a fracture criterion for metal powder compact during the cold compaction process. Based on the fracture criterion of granular materials in compression, a displacement based finite element model has been developed to analyse fracture initiation and crack growth in iron powder compact. Estimation of fracture toughness variation with relative density is established in order to provide the fracture parameter as compaction proceeds. A crack initiated from the boundary of iron powder compact is considered in this work. The finite element simulation of the crack propagation reveals that crack propagates in the direction of higher shear stress and higher relative density. This also implies that the crack grows in the direction where the compaction pressure is much higher, which is in line with the conclusion made by previous researchers on shear crack growth in materials under compression.

Keywords: *Powder compact, Fracture criteria, Fracture toughness, Finite element.*

Introduction

Powder metallurgy (PM) is widely applied to produce mainly automotive parts such as bearings, cams and toothed components. Manufacturing parts using PM involves four major steps: powder and lubricant mixing, compacting powders into appropriate shapes in closed dies to produce green compacts, sintering the green compacts at elevated temperature and finally, post-sintering secondary operations [1, 2].

In modelling the compaction process, the macro-mechanical modelling approach is used in this work, which provides information on the macroscopic behaviour of the powder assembly such as powder movement, density distribution, stress state and the shape of the compact during and after compaction. Thus, the powder medium is considered as a continuum that undergoes large elastic-plastic deformation. In order to describe the effect of stress state on the response of the powder material, constitutive model based on granular material is used since it was found in the literature that powder behaves similarly to a frictional granular material with regard to dilatancy and densification behaviour [3]. Details on cold compaction process can be found in [4], where the numerical modelling of the complete cycle (compaction, relaxation, ejection and emergence) has been developed, and validated by experiments.

Modelling of fracture and crack propagations involves suitable fracture criterion and numerical model to represent the crack propagation process. Even though methods for crack detection in green powder metallurgy (PM) parts exist [5, 6], to date the crack propagation during the compaction process is unknown and needed to improve the performance of parts produced by this process. In this paper a suitable fracture criterion for metal powder during cold compaction process is outlined, taking into accounts the mechanical behaviour of metal powder under compaction process. Finite element modelling of the crack propagation is presented and compared with the findings of previous researchers on crack propagation in materials under compression.

Fracture Criteria

A large number of inhomogenities due to soft and hard inclusions such as voids, pores and microcracks in heterogeneous brittle materials like rock, concrete and ceramic may be the reason for the macroscopic mode II failure under compressive loads in such materials. Similarly, during the compaction process, inhomogenities within the powder compact and frictional behaviour of powder under compaction will obviously expected to lead to macroscopic failure in mode II.

Since powder behaves similarly to frictional granular materials like rock, it is believed that fracture criteria of rock, is most likely the best criteria that can be applied to fracture of powder compact during the compaction process. Based on the fracture of rock, there are two fracture criteria available in the literature that can be applied to powder compact.

Shear Fracture Criterion

Based on the examination of Mode I and Mode II stress intensity factors on the arbitrary plane θ in Figure 1, $K_I(\theta)$ and $K_{II}(\theta)$, varying with θ ($-180^o \leq \theta \leq +180^o$), no matter what kind of loading condition is applied, the shear fracture criterion [17] is expressed as:

$$\frac{K_{II\max}}{K_{I\max}} > \frac{K_{IIC}}{K_{IC}} \quad \text{where } K_{II\max} = K_{IIC} \quad at \;\; \theta_{IIC} \tag{1}$$

Otherwise, crack will propagate as mode I if:

$$1 < \frac{K_{II\max}}{K_{I\max}} < \frac{K_{IIC}}{K_{IC}} \quad \text{where } K_{I\max} = K_{IC} \quad at \;\; \theta_{IC} \tag{2}$$

where $K_{I\,max}$ and $K_{II\,max}$ are maximum stress intensity factors of Mode I and Mode II respectively, while K_{IC} and K_{IIC} are critical stress intensity factors of Mode I and Mode II.

For a crack length of *2a* subjected to a uniform compressive stress, σ and taking into account the shear stress components, the variation of stress intensity factors with θ can be calculated as follows:

$$K_I(\theta) = K_I(0)\cos^3\frac{\theta}{2} + K_{II}(0)\left(-\sin\frac{\theta}{2}\cos^2\frac{\theta}{2}\right) \tag{3}$$

$$K_{II}(\theta) = K_I(0)\sin\frac{\theta}{2}\cos^2\frac{\theta}{2} + K_{II}(0)\cos\frac{\theta}{2}\left(1 - 3\sin^2\frac{\theta}{2}\right) \tag{4}$$

where $K_I(0)$ and $K_{II}(0)$ are the mode I and mode II stress intensity factors in the original crack plane.

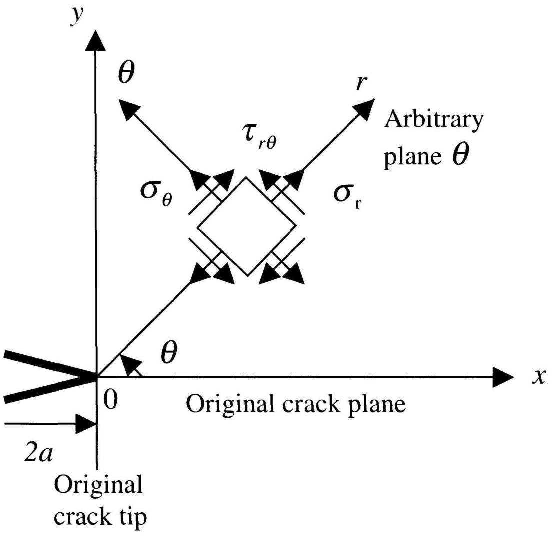

Figure 1: Stress Component at a Point Near a Crack Tip in the Polar Coordinate System

Maximum Shear Stress Criterion

An extension of the maximum tangential stress criterion has been proposed in [7], for the initiation of shear crack in rock under compression. This criterion is analogous to tensile crack initiation, but the direction and stress level of crack initiation are determined by the direction and magnitude of the maximum shear stress. It stated that:

a) A shear crack will initiate when the maximum absolute shear stress computed at a distance $r = r_0$ from the tip reaches a critical value, i.e:

$$\left(|\tau|\right)_{\text{maximum}}\Big|_{r=r_0} = \left(|\tau|\right)_{crit}\Big|_{r=r_0} = \tau_{crit} \tag{5}$$

b) and will initiate in a direction in which absolute value of the shear stress computed at a radial distance $r = r_0$ attains a maximum, i.e:

$$\left.\frac{\partial|\tau|}{\partial\theta}\right|_{r=r_0} = 0 \quad \text{and} \quad \left.\frac{\partial^2|\tau|}{\partial\theta^2}\right|_{r=r_0} < 0 \tag{6}$$

The critical value of absolute shear stress is material dependent, and the radial distance r_0 is viewed as the size of the core region which also called a process zone or plastic zone, that is a zone where the material has yielded.

Finite Element Modelling of Fracture in Powder Compact

Extensive literature reviews on materials under compression reveal that generally crack grows in mode II, no matter whether the material is brittle [8-12] or ductile [13-16]. However, crack patterns are being influenced by the amount of applied stress, and friction between the crack surfaces. Basically, it can be concluded that crack can grow in three different manners:

i) via incipient kink by opening mode, at an angle from the original crack plane
ii) as a closed crack, straight ahead from the original crack plane
iii) as a combination of (i) and (ii)

As compaction proceeds, powder will undergo large deformation, large inhomogeneous density distribution present within the powder compact, while inter-particle frictions as well as friction between powder particle and die wall exist. The combination of (i) and (ii) as stated above are possible for metal powder under compaction as the normal and shear stress acting on the powder increases, while the density distribution keep changing. Since the area of plastic region is difficult to be obtained during compaction process, fracture criterion by [17] as stated in the previous section is simpler and possible to be applied. Therefore, this shear fracture criterion is adopted in this work.

A displacement based finite element procedures have been developed to simulate the powder compaction and fracture process. Mohr-Coulomb yield criterion is used in this work and FORTRAN programming language is used in developing the finite element procedures.

Geometry and Boundary Conditions of Finite Element Model

A multi level component, in this case a rotational-flanged component, is modelled by an axisymmetric representation as shown in Figure 2 and Figure 3. Iron powder with material properties as listed in [18] is compacted by bottom and top punch movements. Total displacement of the bottom punch, $d_b = 7.69$ mm while the top punch, $d_t = 6.06$ mm at the end of compaction process. In this work, the compaction is performed in 20 steps movement of bottom and top punch respectively, and in turn as shown in Figure 3. This mean that a total displacement of 7.69 mm is first achieved when the bottom punch had finished a 20 steps movement (step 1 to 20), followed by a total displacement of 6.06 mm by the top punch after a 20 steps movement (step 21 to 40).

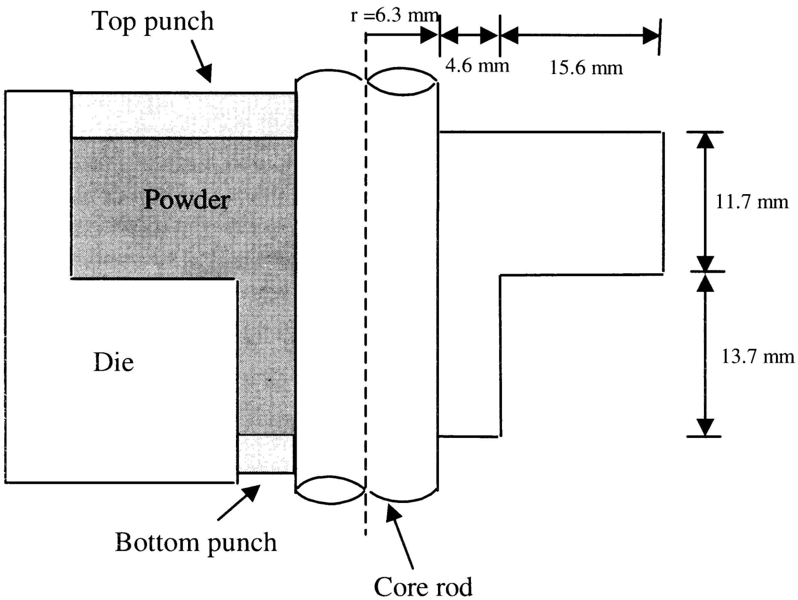

Figure 2: Geometry and Boundary Conditions of a Rotational Flanged Component

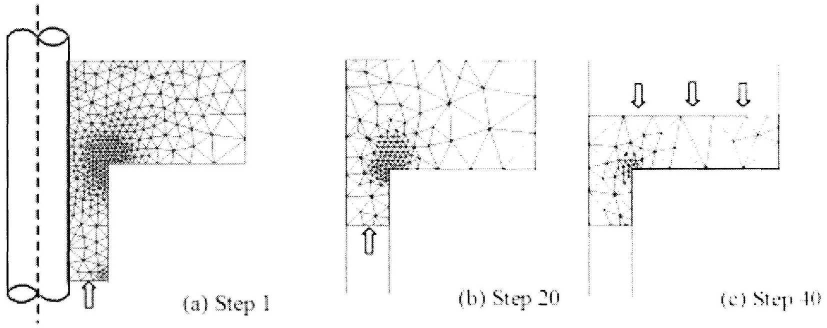

Figure 3: Axisymmetric Representation of Compaction Process at (a) Step 1, (b) Step 20 and (c) Step 40

Adaptive Mesh and Crack Mechanism

An adaptive finite element mesh is applied to accommodate large displacement changes in geometry of the domain. Error estimator based on stress error norm [19] is used, where automatic remeshing is calculated at each step during the compaction process. Crack initiation and propagation have been developed and implemented in the model, without having to predefine the direction of crack. Initially, three nodes triangle element is used. After the first stage of remeshing, the three nodes elements are automatically changed into six nodes triangle elements to have better accuracy.

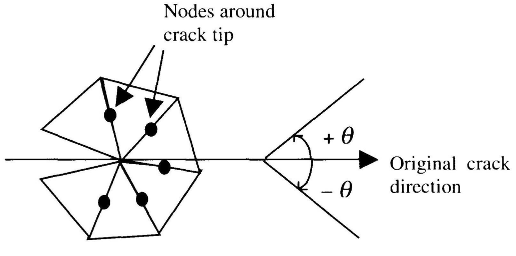

Figure 4: Nodes Around Crack Tip for Calculation of K_I and K_{II}

Calculation of Stress Intensity Factor (SIF)

Equations (3) and (4) are used to calculate the variation of stress intensity factor (SIF) of mode I, $K_I(\theta)$ and mode II, $K_{II}(\theta)$. These values are calculated on the nodes around the crack tip, as illustrated in Figure 4.

The criterion in equation (1) stated that crack occurs when the ratio of maximum K_{II} over K_I exceed the ratio of critical values or fracture toughness, of

K_{II} over K_I. Since no pre-crack is present in this case, the direction of maximum shear stress is used as the original crack direction, in the calculation of K_{II} and K_I for the first crack formation. This is acceptable because the same conclusions regarding the crack path are achieved in materials under compression, by assuming that crack grows along the plane of maximum shear stress and follows the direction of maximum K_{II} [11]. Without pre-crack in this work, the point with maximum shear stress is taken as the point where the crack starts.

Crack Mechanism

In this work, crack is assumed to propagate by an extremely small opening, which is quickly being closed as compaction proceeds. In finite element modelling using advanced remeshing technique, crack propagation can be modelled by inter-element or intra-element in the mesh [20]. Since the values of $K_I(\theta)$ and $K_{II}(\theta)$ are calculated on the nodes around the tip, crack is modelled to propagate inter-element, by splitting mechanism of crack tip node. This is similar to the release node mechanism except that the direction of crack propagation is depending on direction criteria. Referring to Figure 5, the crack tip node is split into two new nodes by adding an extremely small gap if the crack criteria is fulfilled.

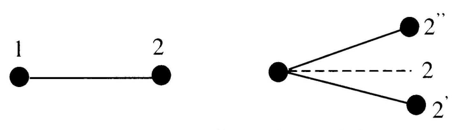

Figure 5: Split node model

Friction Criteria

When two surfaces are in contact, a criteria defining tangential stick or slip occurrence is needed. In general, friction criteria between two surfaces can be stated as:

$$F_f(\tau, \sigma_n) = \begin{cases} < 0 & \text{stick} \\ = 0 & \text{slip} \end{cases} \tag{7}$$

Coulomb friction law which is often adopted in friction problems is used in this work, given by:

$$F_f(\tau, \sigma_N) = |\tau| + \mu\sigma_N \tag{8}$$

where τ is the friction shear stress, σ_N is the normal stress which should be compressive for friction to developed, and μ is the coefficient of friction.

Six nodes isoparametric elements are used as interface elements for friction between powder material and die wall during the compaction process. Details on constitutive model of friction based on plasticity which is incorporated into the interface elements, can be found in [4]. The interface elements are also used to model friction on the crack faces in contact. Using adaptive finite element mesh, the interface element can be inserted automatically on the crack faces, whenever a crack starts and grows.

Fracture Toughness

The fracture criterion in equations (1) and (2) require values of the critical stress intensity factors, K_{IC} and K_{IIC} which are the material parameters and also called fracture toughness. Standard procedures exist for determination of fracture toughness for solids, such as three point bending test or four point bending test. However, fracture toughness of powder compact during compaction process is not as simple as solids due to continuous changing of density and other material properties at each compaction step. Thus, the variation of fracture toughness with relative density must be obtained in order to provide these fracture parameters as compaction proceed.

Mode I Fracture Toughness (K_{IC})

Based on approximate formulas for mode I fracture toughness (K_{IC}) by [21], finite element models have been developed by [22] to estimate the variation of K_{IC} as a function of solidity of carbon foam. By assuming that the crack is parallel to one of the principal material axes, K_{IC} can be estimated using the following formula:

$$K_{IC} = \frac{\sigma_{US}}{\sigma_{\max}} \tag{9}$$

where σ_{US} is the ultimate strength of the material and $\sigma_{\max}$ is the maximum principal stress.

Study on mechanical properties of iron compact has been carried out by [23]. Three point bending tests have been performed on iron compacts, which provide the variation of green strength with relative density, as shown in Figure 6.

Using the variation of green strength in Figure 6 and by assuming that green compact behaves as foam metal, where open and closed porosity in green compact are corresponding to open and closed cells in foam, equation (9) hence becomes:

$$K_{IC} = \frac{148.66\rho' - 65.627}{\sigma_{\max}} \tag{10}$$

where ρ ' is the relative density of the iron compact with respect to solid iron, and σ_{max} is the maximum principal stress.

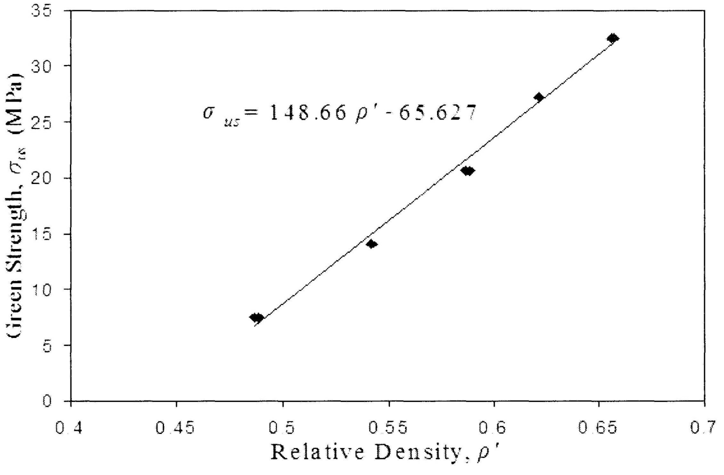

Figure 6: Variation of Green Strength with Relative Density

Mode II Fracture Toughness (K_{IIC})

Fracture toughness of a material is basically the amount of energy a material can absorb before fracture, or energy required to create new crack surfaces. Thus, it is also equal to the area under stress-strain curve up to fracture. Experimental data by [24] is used in this work to obtain the shear stress-strain curves at different compaction load as shown in Figure 7. These curves are subsequently used to estimate the variation of mode II fracture toughness (K_{IIC}) with relative density, as depicted in Figure 8. From Figure 8, the values of K_{IIC} as compaction proceeds can be obtained from:

$$K_{IIC} = 0.1174e^{6.5031\rho'} \tag{11}$$

where ρ 'the relative density of iron compact as in equation (10).

Since the crack is predicted to follow the direction of $K_{II\,max}$, the relative density at the point with maximum K_{II} around the crack tip is used in the calculation of both K_{IC} and K_{IIC}.

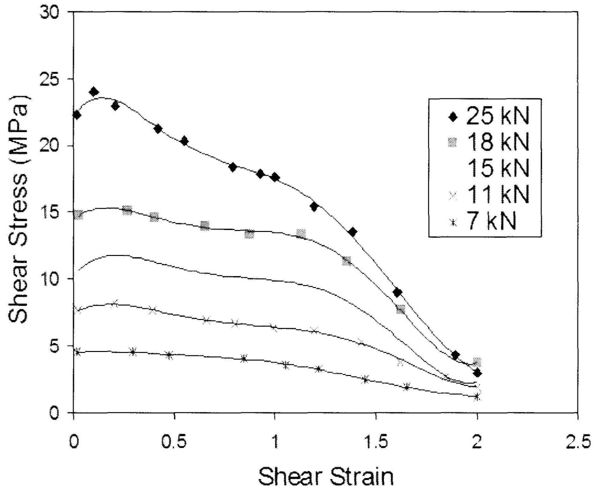

Figure 7: Shear Stress-Strain Curves at Different Compaction Load

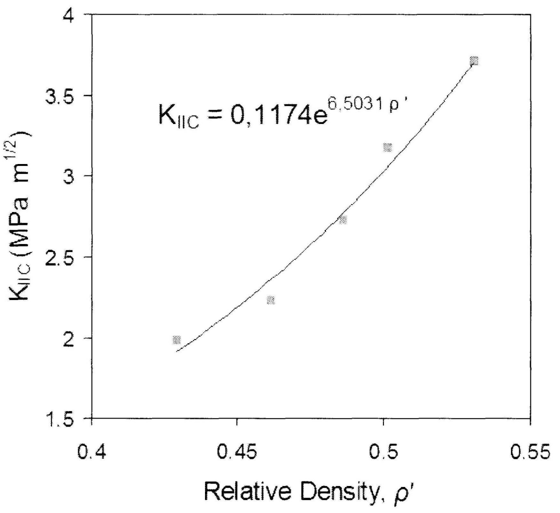

Figure 8: Variation of K_{IIC} with Relative Density

Results and Discussion

Crack Initiation

A single crack propagating inward from the boundary surface is considered in this work. It is found that the point with the maximum shear stress is always generated around the sharp corner as shown in Figure 9. Crack starts at the end of compaction in Step 9, and the shear stress distributions as well as the relative density distributions at Step 10 are shown in Figure 9 and Figure 10 respectively. From these two Figures, it can be seen that crack starts in the region with high shear stress but low relative density.

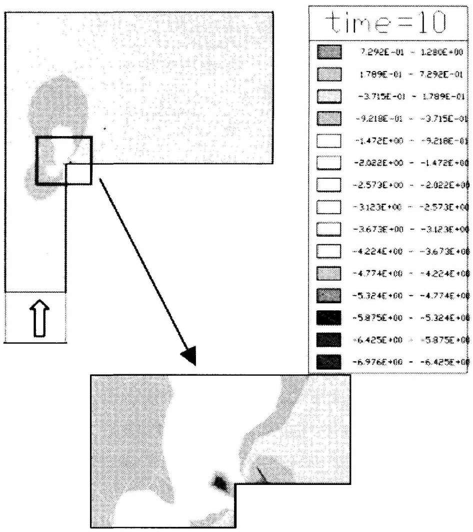

Figure 9: Shear Stress Distribution at Step 10

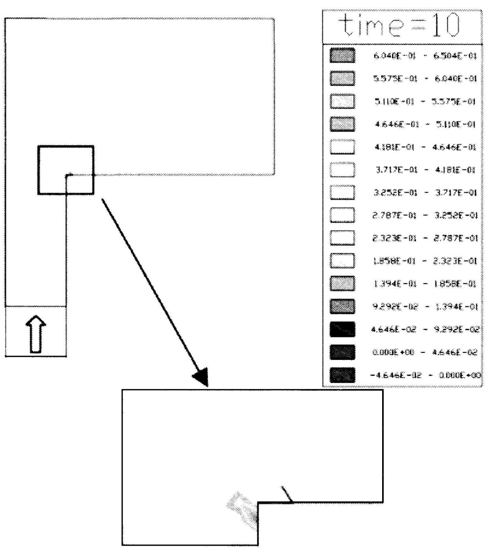

Figure 10: Relative Density Distribution at Step 10

Crack Propagation

As compaction proceeds, the crack propagates at step 17, 18 and 20, where the crack propagation directions, θ at these steps are shown in Table 1. No further propagation occurs after step 20, until compaction is completed at step 40.

Table 1: Crack Propagation Direction

Compaction Step	θ^{o}
17	+22.7883
18	+5.34889
20	+13.74237

The value of θ is calculated with respect to the earlier crack direction, using the sign convention as shown in Figure 4. These values of θ as listed in Table 1 show that the crack always extended away from the original crack direction. Based on the general agreement between the previous researchers, this means that the confining pressure or in this case the compaction pressure, causes the crack to propagate microscopically in opening mode, even though the macroscopic failure is due to mode II fracture. The crack propagation direction however, is much nearer to the original crack plane compared to crack propagation direction when crack extended via a kink by opening mode in materials under compression.

The shear stress distributions and relative density distributions at step 21 are shown in Figure 11 and Figure 12 respectively. Neglecting the sign convention which indicates the direction of stresses, it can be seen from Figure 11 that the crack propagates towards the region with higher shear stresses. Figure 12 shows that the crack also propagates in the direction where the relative density is much higher. Since relative density increases as compaction pressure increases [23, 24], it can be deduced that the crack grows in the direction of higher compaction pressure. This is in line with the conclusion made by [15] which argue that crack grows in the direction of higher confining hydrostatic pressure, which is equivalent to the compaction pressure in this case.

Due to the movement of the bottom punch in the first 20 steps, the two regions with the highest and lowest relative density are formed around the sharp corner as shown in Figure 12. The relative density or compaction pressure gradient around the sharp corner causes the crack to propagate in such direction as in Figure 12. Furthermore, the shear stresses which are initially higher at the boundary as shown in Figure 9 become much lower as compaction proceeds, while the region with higher shear stresses is formed slightly centred, near the sharp corner as in Figure 11. As the consequence, the crack propagates inward starting from the boundary, towards the region where the shear stresses are much higher.

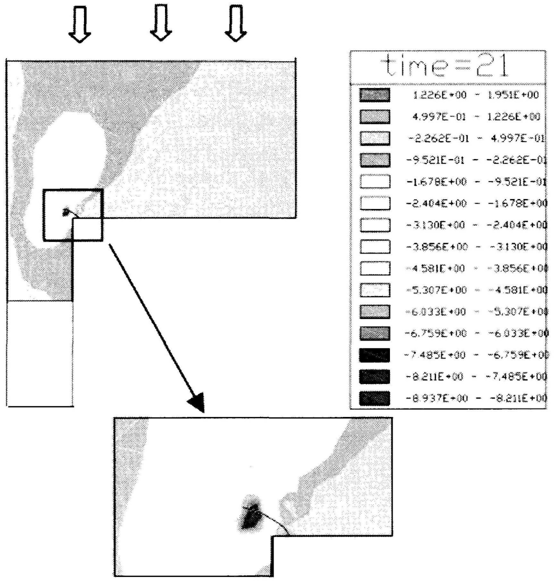

Figure 11: Shear Stress Distribution at Step 21

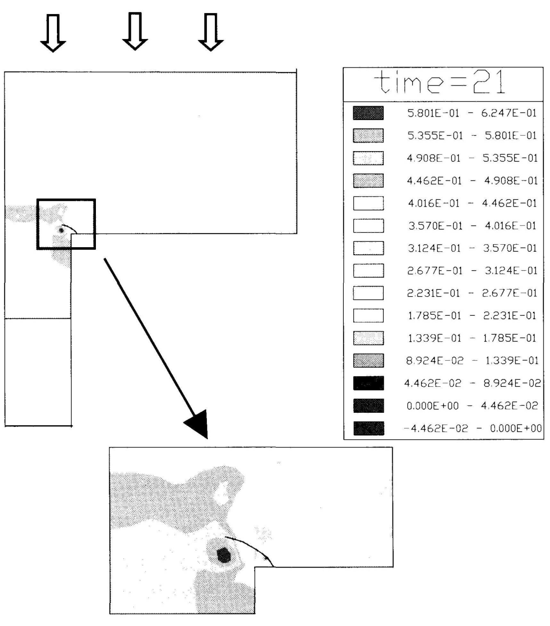

Figure 12: Relative Density Distribution at Step 21

Conclusion

A displacement based finite element model has been developed to simulate the crack initiation and propagation in a rotational flanged component made of iron powder. A fracture criterion of mode II based on fracture of granular materials in compression has been successfully used to model the crack propagation process. Simulation of the crack propagation process in the iron compact reveals that crack starts in the region with the highest shear stress and the lowest relative density distributions. As compaction proceeds, the crack propagates in the direction where the shear stress and the relative density are much higher. Propagation of the crack towards the region of much higher relative density distribution also implies that the crack grows in the direction of higher compaction pressure, which is in line with the conclusion made by previous researchers on crack growth in materials under compression.

References

[1] Chtourou, H., Guillot, M. & Gakwaya, A. (2002). "Modelling of the metal powder compaction process using the cap model. Part 1: Experimental material characterisation and validation". International Journal of Solids and Structures 39, 1059-1075.

[2] Mori, K., Sato, Y., Shiomi, M. & Osakada, K. (1999)."Prediction of fracture generated by elastic recoveries of tools in multi-level powder compaction using finite element simulation". Int. J. of Machine Tools & Manufacture 39, 1031-1045.

[3] Gollion, J., Bouvard, D. & Stutz, P. (1989)."On the rheology of metal powder during cold compaction". Proc. Int. Conf. Micromechanics of Granular Media, Powder and Grains. Ed. J. Biarez and R. Gourves, 433-438.

[4] Ariffin, A. K. (1995). "Powder compaction, finite element modelling and experimental validation". PhD Thesis. University of Wales Swansea, United Kingdom.

[5] Hauck, E. T., Rose, L. J. Won-Joon, S. & Heaney, D. F. (2003). "A surface wave mediator technique for crack detection in green parts". Proceeding of The 2003 International Conference on Powder Metallurgy & Particulate Materials.

[6] Frederick, K., Zetec, Inc. (2003). "Eddy current testing of powder metal components". www.zetec.com/documents/pwdr_met_insp(1).pdf.

[7] Bobet, A. (2000). "The initiation of secondary cracks in compression". Engineering Fracture Mechanics 66, 187-219.

[8] Melin, S. (1986). "When does a crack grow under mode II conditions?". Int. Journal of Fracture 30, 103-114.

[9] Melin, S. (1987). "Fracture from a straight crack subjected to mixed-mode loading". Int. Journal of Fracture 32, 257-263.

[10] Mao, H. Y., Zan, Y. W., Zhao, J. & Yoshimine, M. (2002). "A unified strength criterion for rock material". Int. Journal of Rock Mechanics & Mining Science 39, 975-989.

[11] Isaksson, P. & Stahle, P. (2002). "Mode II crack paths under compression in brittle solids -A theory and experimental Comparison". International Journal of Solids and Structures 39, 2281-2297.

[12] De Bremaecker, J.Cl. & Ferris, M.C. (2004). "Numerical models of shear fracture propagation". Engineering Fracture Mechanics 71, 2161-2178.

[13] Liu, A.F. (1974). "Crack growth failure of aluminium plate under in-plane shear". AIAA Journal 12, 180-185.

[14] Hallback, N. (1998). "Mixed mode I/II fracture behaviour of high strength steel". International Journal of Fracture 87, 363-388.

[15] Roy, Y. A., Narasimhan, R. & Arora, P.R. (1999). "An experimental investigation of constraint effects on mixed mode fracture initiation in a ductile aluminium alloy". Acta Mater. 47, 1587-1596.

[16] Isaksson, P. & Stahle, P. (2003). "A directional crack path criterion for crack growth in ductile materials subjected to shear and compressive loading under plane strain conditions". International Journal of Solids and Structures 40, 3523-3536.

[17] Rao, Q., Sun, Z., Stephansson, O., Li, C. & Stillborg, B. (2003). "Shear fracture (mode II) of brittle rock". Int. Journal of Rock Mechanics & Mining Sciences 40, 355-375.

[18] Tran, D.V., Lewis, R.W., Gethin, D.T. & Ariffin, A.K. (1993). "Numerical modelling of powder compaction process: displacement based finite element method". Powder Metallurgy Vol. 36, No. 9, 257-266.

[19] Zienkiewicz, O.C & Zhu, J.Z. (1989). "Error estimates and adaptive refinement for plate bending problems". Int. Journal for Numerical Methods in Engineering. 28, 2839-2853.

[20] Bouchard, P.O., Bay, F., Chastel, Y. & Tovena, I. (2000). "Crack propagation modelling using an advance remeshing technique". Comput. Methods. Appl. Mech. Engineering 189, 723-724.

[21] Gibson, L.J. & Ashby, M.F. (1998). "Cellular solids: structure and properties." 2nd ed. (Cambridge University press, United Kingdom).

[22] Choi, S. & Sankar, B.V. (2003). "Fracture toughness of carbon foam". Journal of Composite Materials. 37(23), 2101-2116.

[23] Poquillon, D., Baco-Carles, V., Tailhades, P. & Andrieu, E. (2002). "Cold compaction of iron powders-Relations between powder morphology and mechanical properties Part II. Bending tests: results and analysis". Powder Technology 126, 75- 84.

[24] Jumahat, A. (2001). "Analysis of thermo-mechanical behaviour of warm compaction process" (In Malay language), Master of Science Thesis. Universiti Kebangsaan Malaysia, Malaysia.

S.M. TAHIR, A.K. ARIFFIN & N. MUHAMAD, Computational Mechanics Laboratory, Department of Mechanical & Materials Engineering, Universiti Kebangsaan Malaysia, 43600 Bangi, Selangor.